

# Electron Energy States of InAs/GaAs Quantum Ring Array

I. Filikhin\*, E. Deyneka\*\*, G. Melikian\* and B. Vlahovic\*

\*Physics Department, North Carolina Central University, 1801 Fayetteville St.  
Durham, NC 27707, USA, branko@jlab.org;

\*\*Center for Advanced Materials and Smart Structures, North Carolina A&T University, Greensboro,  
NC, USA

## ABSTRACT

Planar array of InAs/GaAs semiconductor quantum rings is studied under the single sub-band approach with the energy dependent effective mass. Periodic boundary conditions for the electron wave function are used for the quantum ring array modeling. The 3D nonlinear problem of the confined energy is solved numerically by the finite element method. Mutual influence of the QR's in array is considered by variation of the unit cell range. The results of modeling of the quantum ring electron states are compared with calculations of the other authors, and experimental data.

**Keywords:** quantum ring array, InAs/GaAs heterogenic nanostructure, finite elements method.

## 1 INTRODUCTION

Recent successful fabrication of the self-assembled InAs/GaAs quantum rings (QR) and arrays of quantum rings [1] has demonstrated that these structures have significant potential for practical photonic device applications, as stimulated further experimental and theoretical studies [2-5]. In this paper a model based on the single sub-band approach [6] with the energy dependent effective mass [7-10] is applied to numerical analyze the effect of QR array geometry on energy states of QR. In particular, a mutual influence of the QR's in array is investigated. In order to test the adequateness of this model for the description of real nano-scaled objects (as QR or the array of QR's), a detailed comparison of the calculated spectral properties of single QR with available experimental data and the results of others authors is conducted.

## 2 DECIPTION OF MODEL

Planar array of InAs quantum rings is considered. The quantum rings have a cylindrical shape and are embedded into the GaAs substrate. Geometrical parameters of the QR are height  $H$ , radial width  $\Delta R$  and inner radius  $R_1$  (the outer radius is  $R_2 = R_1 + \Delta R$ ). The unit cell of the QR along with distribution of QRs in array is schematically shown in Figure 1.

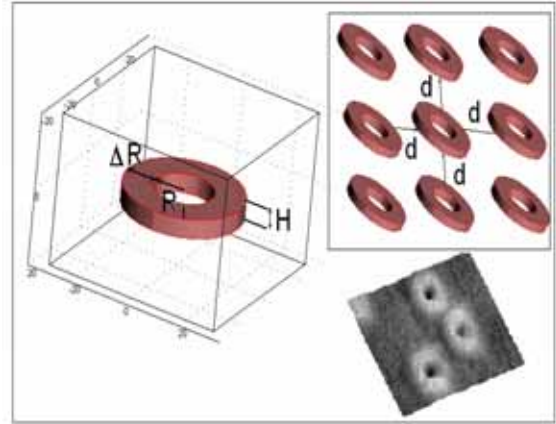


Figure 1: The unit cell of the quantum rings array. The size parameters are defined as shown. The picture of the experimental fabricated QRs is given from [1].

This 3D heterogeneous structure is modeled utilizing the  $kp$ -perturbation single subband approach [6] with energy dependent quasi-particle effective mass. The energies and wave functions of a single electron in a semiconductor structure are the solutions of the nonlinear Schrödinger equation:

$$\left( -\frac{\hbar^2}{2m^*(x, y, z, E)} \nabla^2 + V(x, y, z) - E \right) \psi = 0, \quad (1)$$

where  $V(x, y, z)$  is the band gap potential, proportional to the energy misalignment of the conduction band edges of InAs QR and GaAs substrate. The electron effective mass  $m^* = m^*(x, y, z, E)$  is defined by the Kane formula [7] for each area of QR/Substrate:

$$\frac{m_0}{m^*} = \frac{2m_0 P^2}{3\hbar^2} \left( \frac{2}{E_g + E} + \frac{1}{E_g + \Delta + E} \right). \quad (2)$$

Here  $m_0$  is free electron mass,  $P$  is Kane's momentum matrix element,  $E_g$  is the band gap, and  $\Delta$  is the spin-orbit splitting of the valence band. Inside the QR  $E$  is the ground state confinement energy. In order to take into account the non-parabolic effect on the substrate, we used (2) where  $E$  should be replaced by  $E - V_0$  for the

substrate. Periodic boundary conditions for the wave function  $\Psi$  on the surface side of the QR array unit cell (Fig.1) are chosen to satisfy the relation:  $(\vec{n}, \vec{\nabla}\Psi) = 0$ , where  $\vec{n}$  is the surface normal. The following experimental values [11] are used for the QR (index 1) and the substrate (index 2) components:  $(2m_0P_1^2)/\hbar^2=22.4$ ,  $(2m_0P_2^2)/\hbar^2=24.6$ ,  $E_{g,1}=0.42$  eV,  $E_{g,2}=1.52$  eV,  $\Delta_1=0.34$  eV,  $\Delta_2=0.49$  eV. Bulk effective masses of InAs and GaAs are  $m_{0,1}^*=0.024m_0$  and  $m_{0,2}^*=0.067m_0$ , respectively. The magnitude of  $V_0$  was calculated as  $V_0=0.7(E_{g,2} - E_{g,1})=0.77$  eV.

### 3 RESULTS OF CALCULATIONS

The non-linear Schrödinger equation (1) is solved by the iterative procedure, where the solution of the linear Schrödinger equation for each step is numerically obtained by finite element method. Details of the numerical treatment were described earlier [10].

The results of calculations of the electron ground state energy dependence on the distance between QRs in an array are given in Fig. 2.

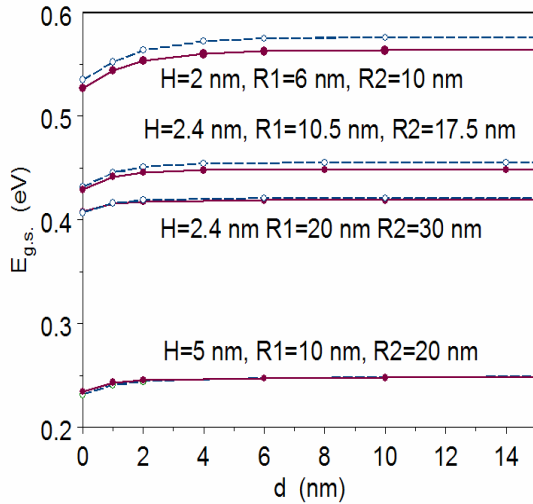


Figure 2. Electron ground state energy as a function of the distance between QRs for various QR size parameters. The calculations with the parabolic (dashed lines) and non-parabolic (solid lines) approximation are shown.

One can see that the magnitude of the mutual influence depends on the value of the confinement energy, and declines quickly in the range of 2-4 nm. It is clear that at the distances larger than these values each QR in the array can be considered as a standing alone single QR. The non-parabolic effect does considerably alter the energy of the electron states, especially when the height and the width of

QR are relatively small. For such cases the effect of non-parabolicity, and the mutual influence of QR's are of the same order.

In Fig. 3 the first several energy levels calculated for different distances  $d$  between the quantum rings are shown. Character of the energy dependence on  $d$  conveys as it was for the ground state. A new effect is the increased shifts of energy for increased numbers of the levels.

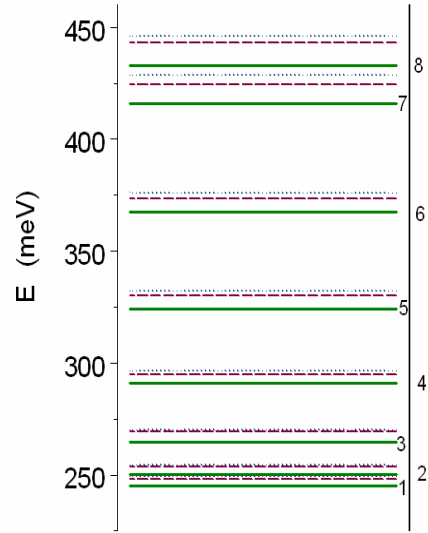


Figure 3. Electron energy spectra of QR ( $H=5$  nm,  $R_1=10$  nm,  $R_2=20$  nm) for different distances  $d$ . Solid lines:  $d=0$  nm; dashed lines:  $d=3$  nm; dotted lines:  $d=10$  nm.

To illustrate our calculations, spatial configurations of the electron density probability function at various distances between the QR's, and at the energies  $E_a$  corresponding to different quantum numbers  $a = (n, l)$ , are depicted in Fig.4 and Fig.5, respectively. In Figure 4 the ground state (0,0) and in Figure 5(a)-(d) the states with quantum numbers (0,0), (0,2), (0,5), (1,0) are shown.

We have compared our QR calculations with the calculations of Li and Xia [8], who applied the formalism of plane wave functions for solution of the Schrödinger equation in similar QR model using the periodic boundary conditions. In that model [8] the periodic boundary conditions correspond to the 3D space array of the cylindrical quantum rings (or the quantum dots) with a large value of unit cell range (in the asymptotical limit  $d \rightarrow \infty$ ; see Fig. 2).

We have calculated the electron ground state energy with corresponding boundary condition for the cylindrical shape InAs/GaAs QR and QD with  $E_g = 0.78456$  eV [8] for InAs ( $E_c=0.513$  eV), as well as non-parabolicity of the conduction band:  $m_i^* = m_b^*(1 + 2E/E_g)$  [8], where  $m_b^*$  is the effective mass of conduction band bottom,  $i = 1, 2$ .

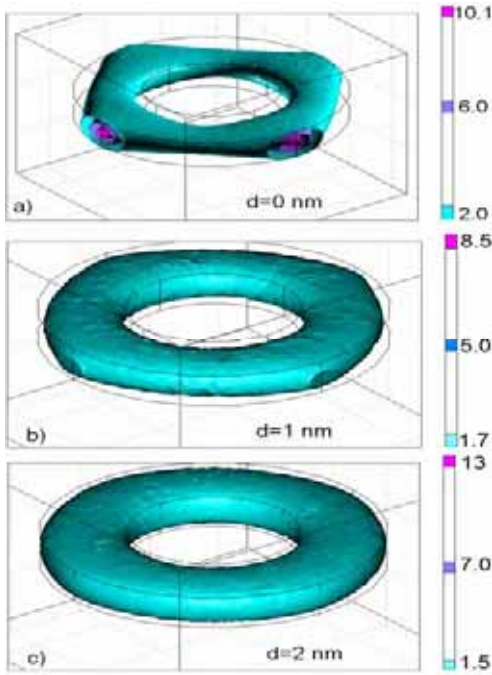


Figure 4. Probability density isosurface for various distances  $d$  between the quantum rings of with  $H=5$  nm,  $R_1=10$  nm,  $R_2=20$  nm.

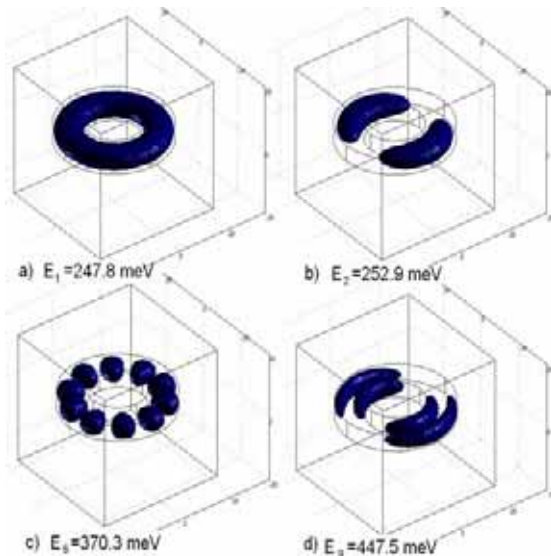


Figure 5. In-cell spatial localization of probability density function for energies corresponding to different quantum numbers  $n$ .  $H=5$  nm,  $R_1=10$  nm,  $R_2=20$  nm,  $d=6$  nm.

Figure 6 represents the results of the above comparison. The electron ground state energy of QR (QD) is shown as a function of width  $\Delta R$  for  $H=1$  nm and  $H=2$  nm. The results of our calculation coincide with [8] for  $H=1$  nm since the height of QR is noted as 2 nm in [8]. Perhaps it is a typing mistake. The next comparison for the electron energy spectra supports this conclusion. In Fig. 7 the results of

calculation of the excitation energy for several levels of single QR (with  $E_c$  from [8] and  $H=1$  nm) are shown. As one can see, our results are in a good agreement with original calculation of [8]. In Fig. 7 the experimental values for the (1, 1) level [4] from [1] are given as well.

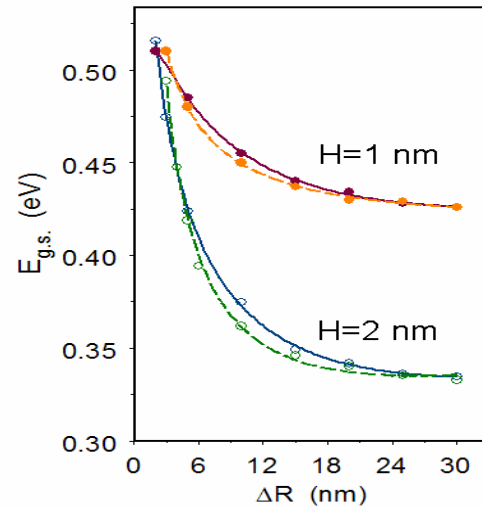


Figure 6. Electron ground state energy of the InAs/GaAs QR (solid lines) and QD (dashed lines) as a function of the width  $\Delta R$  for  $H=1$  nm and  $H=2$  nm ( $R_1=10$  nm for QR and  $R_1=0$  nm for QD). Open and solid circles are the results of the present work and calculations [8], respectively. Our results for  $H=1$  nm coincide with [8] and not shown here.

In [1] a value of the outer radius of QR's is not exactly defined ( $30 \text{ nm} < R_2 < 70 \text{ nm}$ ), and it is about 40 nm in [3]. Calculated energy for  $R_2=45$  nm is different from the experimentally obtained. We have corrected the value of  $R_2$  to 38 nm. This correction allows us to reproduce the experimental excitation energy for the (1,1) state of QR. This state is marked in Fig. 8 as the  $\Delta n = 1$ . States with the main quantum number  $n = 0$  are marked as  $\Delta n = 0$ . In Fig. 8 the result of calculation [4] are also shown, which have been carried out within one dimension model of parabolic confinement potential with effective radius of  $R_0=14$  nm. The electron effective mass of QR in this calculation was chosen as  $0.06 m_0$ . The effect of non-parabolicity, taken into account in our model, leads to a significant change in the electron effective mass of QR in respect to the bulk value (see relation (2)). For the QR considered above effective mass of InAs increases from the initial value of  $0.024 m_0$  to  $0.051 m_0$ , which is closer to the one of GaAs,  $0.059 m_0$ . This value adheres to the electron effective mass of  $(0.057 \pm 0.007) m_0$  observed in [5] for QD.

## 4 CONCLUSION

Planar array of InAs/GaAs quantum rings was studied under the energy dependent effective mass approximation. It is found that the mutual influence of the QR's in array is sufficient when the distances between neighboring QRs are less than 2-4 nm. The magnitude of this effect depends on the confinement energy. It is shown that presented model can adequately describe the QR. In particular, this model allows us to reproduce experimental data for the electron excitation energy of QR. In addition, the observed deviation of QR electron effective mass from its bulk value can be attributed to the non-parabolic effect.

## REFERENCES

- [1] A. Lorke, R. J. Luyken, A. O. Govorov, and J. P. Kotthaus, J. M. Garcia† and P. M. Petroff, Phys. Rev. Lett. 84, 2223-2226, 2000.
- [2] B. Roostaei and K. Mullen, arXiv: cond-mat/0312173.
- [3] A. O. Govorov, S. E. Ulloa, K. Karrai, R. J. Warburton, Phys. Rev. B 66, 081309(R), 2002.
- [4] A. Emperador, M. Pi, M. Barranko, A. Lorke, Phys. Rev. B. 62, 4573-4577, 2000.
- [5] B. T. Miller et al., Phys. Rev. B 56, 7664-6769, 1997.
- [6] J. M. Luttinger and Kohn W. Phys. Rev. 97, 869, 1955; Luttinger J. M. Phys. Rev. 102, 1030, 1956.
- [7] Kane E. Band Structure of Indium Antimonide. Journal of Physics and Chemistry of Solids, 1, 249-261, 1957
- [8] S. S. Li and J. B. Xia, J. Appl. Phys. 89, 3434-3437, 2001.
- [9] Y. Li, O. Voskoboynikov, C.P. Lee., S.M. Sze, O. Tretyak, J. Appl. Phys. 90, 6416-6420, 2002.
- [10] I. Filikhin, E. Deyneka and B. Vlahovic, Modelling Simul. Mater. Sci. Eng. 12, 1121-1130, 2004.
- [11] Handbook Series on Semiconductor Parameters, edited by M. Levinshtein, S. Rumyantsev and M. Shur, (World Scientific, Singapore) 1999.

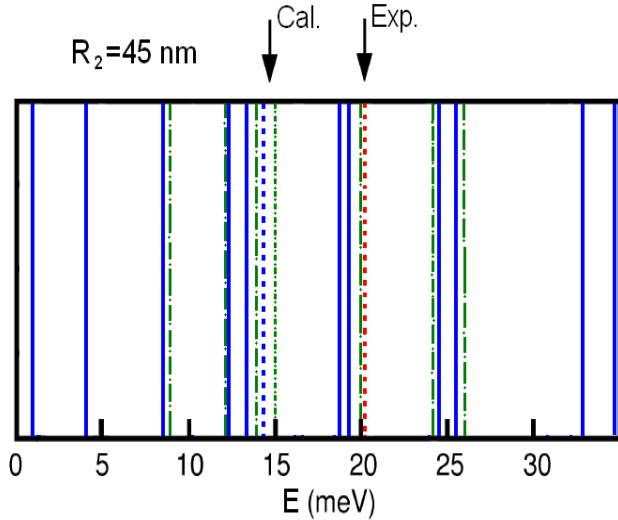


Figure 7. Excitation energy of the electron states for QR with  $H=1$  nm,  $R_1=10$  nm,  $R_2=45$  nm. For  $\Delta n = 0$  case the solid lines correspond to our calculation within the model of [8]. Original values of [8] are defined by the dot-dashed lines. For  $\Delta n = 1$  calculated and experimental values [1] are depicted by the short dashes and arrows on the top of figure, respectively.

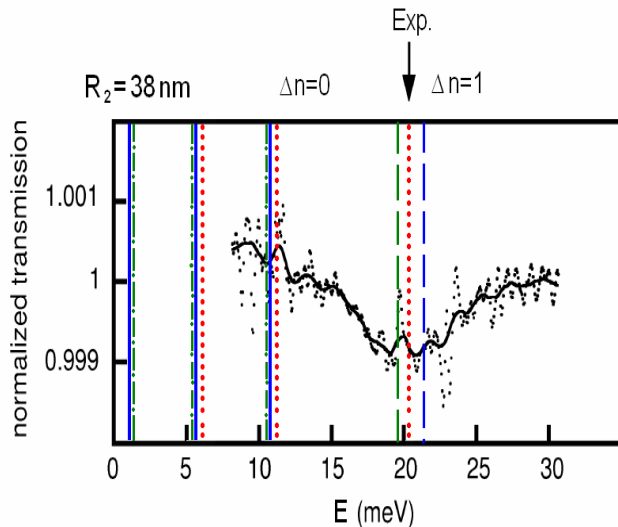


Figure 8. Excitation energy of the electron states for QR with  $H=1$  nm,  $R_1=10$  nm,  $R_2=30$  nm. Calculated values are denoted by the solid lines for  $E_c=0.77$  eV, and the dot-dashed lines for  $E_c=0.513$  eV. The values calculated in [4] are shown by the dotted lines. The solid curve is the fit of the experimental data from [1] for electron transmission. Transmission minimum (noted by arrow) relates to the electron energy level with  $\Delta n = 1$ . The first three energies correspond to the  $\Delta n = 0$  transitions.